Proceedings of 2004 IEEE/RSJ International Conference on
Intelligent Robots and Systems
September 28 - October 2, 2004, Sendai, Japan

An anthropomorphic robot torso for imitation: design and experiments

Manuel Lopes Ricardo Beira Miguel Praça José Santos-Victor

Instituto de Sistemas e Robótica
Instituto Superior Técnico
Lisboa, Portugal

Escola Superior de Tecnologia
Instituto Politécnico de Setúbal
Setúbal, Portugal

http://vislab.isr.ist.utl.pt
{jasv,macl}@isr.ist.utl.pt

***Abstract*— We describe the design of an anthropomorphic robot, combining a binocular head, an arm and a hand, for research in visuomotor coordination and learning by imitation. Our goal was to produce a system resembling the human arm-hand kinematics as closely as possible, while keeping it simple and relatively low-cost. We present mechanical details, kinematics and sensors together with a discussion of the main design options. We present results with human-arm coordination, as well as imitation of a human demonstrator, in real time.**

I. Introduction

Research in imitation, skill transfer and visuomotor coordination have become increasingly important in the past few years, partly motivated by the advances in computing power and knowledge about vision or motor control in biological systems, and pushed by applications like service robotics or robot companions. However, such research efforts are often undermined by the unavailability of adequate, hand-eye-head robotic research platforms.

The goal of this paper is two-fold. On one hand, we describe the design procedure (and final result) of a humanoid robotic torso combining an anthropomorphic arm, hand and binocular head (Figure 1), driven by the research needs. On the other hand, we show preliminary results on imitation learning with this system.

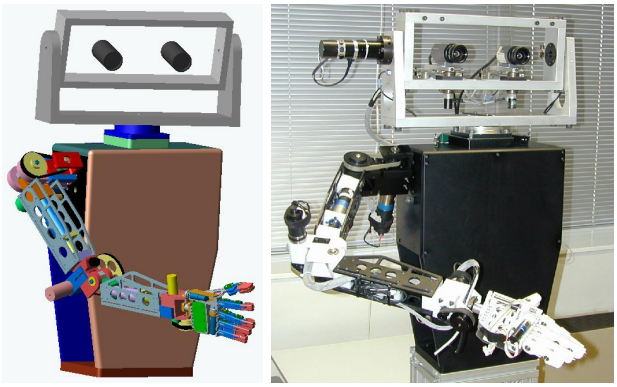

Fig. 1. Cad Model and real robot

Ever since the 60's, when the first robotic arms appeared, the development of new systems has never stopped. The *PUMA* is perhaps the most widely known robot arm, with 6 degrees of freedom and it is extremely robust. However, the control architecture is closed, the cost is relatively high for many research labs, the controllers (and power amplification) are quite large and only a simple gripper is available. There are other systems in the market, with lower cost and size. For example, the *KATANA* [1] is a small manipulator, with an open architecture but it only has 5 degrees of freedom and a simple gripper.

With the increasing interest in humanoid robots, many different arm and hand designs have been suggested. The design varies quite significantly according to the desired use for these robots. Humanoid torsos, comprising arms and head, have been used to study head/arm coordination [2], [3], [4]. For legged robots there are several topics for research. These robots must generate the necessary torques to carry their own weight [5], [6]. Some of these robots may be able to fall down and stand-up by themselves. Other robots are designed to study human locomotion [7], [8].

It is known that for a stable grasp we need at least 3 fingers, which is the reason why most robotic hands contain 3 fingers. The kinematics of *Shadow* [9] resembles that of the human hand, with 21 degrees of freedom (DOFs). Other projects tried to achieve the same number of degrees of freedom, but not all of them can be controlled independently. The Karlsruhe[10] hand has 20 DOFs, actuated by a single motor. The rationale of the design is that the exact position of each finger is not important, when grasping objects in different ways. If the hand can automatically (passively) adapt to the object shape, then stable grasp can be achieved with minimum computation. Another robot hand with 13 degrees of freedom is described in [11].

There are some works using robots to study imitation. Imitation is believed to be an important path towards autonomous humanoid robotics [12]. In [13] the movements of a person are tracked with a stereo camera using markers. Then, the full-body imitation is achieved through iterative optimization to solve the inverse kinematics. The work described in [14] modeled several components of the brain, presumably involved in imitation. This work was extended for the case of grasp recognition (mirror neurons) [15] and an implementation with video data was used. Although good results were obtained, the

0-7803-8463-6/04/$20.00 ©2004 IEEE

visual features used are very difficult to extract, which makes it difficult to use in real world conditions. For the case of learning motor skills, [16] presents a biologically motivated architecture. This systems works with real data and learns repetitive patterns and precise movements for grasp and reaching. Several other works used biological principles in order to achieve imitation [17].

The long-term goal of our research consists in developing methodologies whereby and artificial system can learn to perform new tasks by observing other robots or human tutors. The ability to understand and perform human-like gestures is therefore of the utmost importance, and constitutes the fundamental constraint for our design.

Hence, our design of a human-like robotic torso, consisting of a head, arm and hand, was driven by the following constraints:

- The robot kinematics should resemble that of the human torso. It should be able to perform human-like movements and gestures, as well as to allow a natural interaction with objects (e.g. while grasping).
- Payload of at least $500grs$ (with the hand).
- Force detection should be possible.
- Ease of maintenance and low-cost.

The constraint on the kinematics basically precludes the usage of commercially available systems. Most standard robot arms, like the PUMA, have the first 3 degrees of freedom (base azimuth, elevation and elbow elevation) to position the end effector in space, while the last 3 DOFs (in the wrist) allow the control of orientation. One important movement in the human arm is the rotation around the upper arm, that one cannot find in commercial systems. This movement enables the arm to better deal with obstacles and comfort, when manipulating (e.g. writing with the arm standing on a table compared to writing on a black board), and leads to more natural movements. Our robot arm is able to perform rotations around the upper arm. Although we have only two degrees of freedom in the wrist, combined with the DOFs available in the hand we get sufficient dexterity.

The Karlsruhe hand design has the attractive feature of allowing full adaptation to object's shape, while using just a single motor. We followed a similar concept to reduce the number of actuators, by keeping some degrees of freedom in the hand coupled. One important limitation with the Karlsruhe hand is that it cannot perform hand gestures, since the different fingers cannot be controlled independently. For closing some fingers independently, some DOFs must be decoupled.

Our hand has eleven degrees of freedom, that are controlled by four motors included in the hand. With this choice, our robot hand can adapt passively to the shape of objects but it can also perform a number of hand gestures that a simpler design would not allow. Thus, our design represents a tradeoff between simplicity and multi-purpose use. We show that several objects can be grasped: sphere, box, cylinders and general geometric shapes. With its four independent controllers it is also possible to perform the most significant hand gestures.

Since our anthropomorphic arm-hand will be in contact with objects in the world, it is necessary to be able to sense forces acting upon the system. We chose motor controllers with this capability. In every movement, the arm motor is limited to a maximum torque (current). For the hand, we also installed force sensors in the fingers pulp and palm to better control the exact contact forces.

The usage of standard components, whenever possible, has an important impact on the overall cost of actually producing the system, an important constraint for many research groups. We used regular DC motors with reduced backlash and off-the-shelf mechanical parts. The robot structure was machined in a workshop at our institute.

The arm can be assembled or disassembled easily. The overall design involved several iterations between design, analysis of specifications and prototyping. We are now obtaining the first results and we consider that it can be very attractive for other research labs as well.

We will show several properties of our system. The specific kinematics is redundant for positioning the hand. The arm can be coordinated with the head in order to always foveate the hand. Several objects can be grasped in a stable way.

As our goal for constructing this system was imitation we will present results where a person movement is mimicked by the robot. A specific vision system was implemented in order to do this. We developed a system that tracks people in real-time, based on the skin color information, vertical position and static background.

In Section 2, we present the detailed design of the anthropomorphic robot arm. Section 3 is devoted to the design and demonstration of the multi-fingered robot hand. Section 4 describes the binocular robot head used in the torso. Section 5 presents some results on gesture imitation performed with this system and in Section 6, we draw some conclusions and point out directions of future work.

II. Design of an anthropomorphic robot arm

As we mentioned before, our goal is to design a robot arm for conducting research in human-based imitation, learning and visuomotor coordination. For this reason, the arm kinematics must resemble that of humans. In this section, we present an overview of the kinematics of the human arm, followed by the description of our design options and results. Finally we describe the direct and inverse kinematics of our anthropomorphic robot arm. When presenting the inverse kinematics, we will demonstrate some interesting properties of our design.

A. The human arm anatomy

For the sake of completeness of the paper, we summarize here the main facts related to the human arm anatomy. It consists of a synthesis of what can be found in [18].

The human arm is a very complex system. The upper limb is composed of three chained mechanisms, the shoulder girdle, the elbow and the wrist. Considering bones in

pairs, seven joints may be distinguished. Except for the scapulo-thoracic joint, one can neglect the translational movement with respect to rotations, and assume that these joints behave as ball and socket joints, allowing 3 degrees of freedom (DOF) in rotation.

The seven joints can be identified as follows: the sterno-clavicular joint(3 DOF), which articulates the clavicle by its proximal end onto the sternum, the acromio-clavicular joint, which articulates the scapula by its acromion onto the distal end of the clavicle; the scapulo-thoracic joint(5 DOF), which allows the scapula to glide on the thorax; the gleno-humeral joint(3 DOF), which allows the humeral head to rotate in the glenoid fossa of the scapula; the ulno-humeral and the humero-radial joints; which articulate both ulna and radius on the distal end of the humerus, and finally the ulno-radial joint where both distal ends of ulna and radius join together(2 DOF).

To perform these movements, the upper limb is equipped with not less than 21 muscles actuators. Some muscles have very broad attachments, while some others divide in several bundles attached on different bones. These muscles can be classified in several groups according to the bone they move and the DOF they control. As muscles never work in isolation, natural movements always involve the motions of all bones. For a complete analysis, it is necessary to consider the motion of the mechanism as a whole.

B. Robot arm design

From the previous description, it is clear that it would be extremely difficult (if not impossible) to design a robot arm with the exact amazing capabilities of motion of the human arm. For constructing our robot arm, we were forced to introduce some simplifications, yet with the care of maintaining the main functional requirements. The shoulder was modeled with 3 DOF: external/internal rotation, abduction/adduction and extension/flexion. The elbow is endowed with 2 DOF: extension/flexion and supination/pronation. Finally, the wrist possesses 1 DOF: extension/flexion. Wrist abduction/adduction is not included but we will see that it is compensated by the hand.

The following sections describe the arm kinematics.

B.1. Direct Kinematics

In this section we present the computational model for the arm kinematics. The arm is described with the modified Denavitt-Hartenberg parameters [19], shown in Table I. The corresponding axes are illustrated in Figure 2.

The first three joints model the shoulder. The first joint is responsible for abduction/adduction, the second for extension/flexion and the third for external/internal rotation. The fourth joint makes the extension/flexion of the elbow, the fifth the pronation/supination of the fore-arm and the sixth the extension/flexion of the wrist.

B.2. Inverse Kinematics

The inverse kinematics will be done in two parts: position of the wrist and orientation of the hand. Due the particular structure of the arm, an iterative process may be necessary. In most robot arms (e.g. the PUMA), the first 3 links determine the end-effector's position and the last three the orientation. In our arm the third joint contributes both to position and to orientation of the hand.

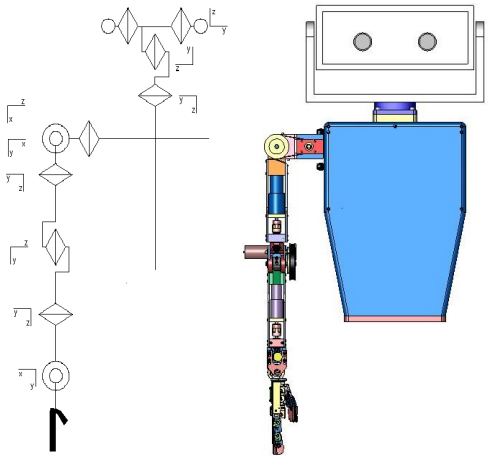

Fig. 2. Kinematic structure for the arm and head.

Joint	a_{i-1}	α_{i-1}	d_i	$\theta_i(deg)$	$limits(deg)$
1	0	0	0	θ_1	[-45 135]
2	0	90	0	$\theta_2 + 90$	[-110 10]
3	0	90	l_1	$\theta_3 + 90$	[-90 0]
4	a_1	90	0	θ_4	[-90 0]]
5	$-a_2$	-90	l_2	$\theta_5 + 90$	[-90 90]]
6	0	90	0	θ_6	[-45 45]

TABLE I

MODIFIED DENAVITT-HARTENBERG PARAMETERS OF THE PRONATOR ARM. ALL ANGULAR VARIABLES ARE EXPRESSED IN DEGREES.

Let P denote the desired position of the wrist, and Z be the null vector. Writing these vectors in homogeneous coordinates, we have:

$$P = [x \;\; y \;\; z \;\; 1]^T \qquad Z = [0 \;\; 0 \;\; 0 \;\; 1]^T$$

The wrist position, P, can be related to the various joint angles by cascading the different homogeneous coordinate transformation matrices:

$$P = \prod_{i=0}^{5} {}^{i}_{i+1}T \; Z \tag{1}$$

where ${}^{i}_{i+1}T$ denotes the homogeneous coordinate transformation between frames $\{i+1\}$ and $\{i\}$. As, in general, most of the terms of this equation are transcendental, we will use the fact that the equation:

$$a\cos(\theta) + b\sin(\theta) = c, \;\; \text{has solutions}$$
$$\theta = 2\arctan\left(\frac{b \pm \sqrt{a^2 + b^2 - c^2}}{a + c}\right) \tag{2}$$

This equation will be useful when determining the joint angles in the inverse kinematics. Notice that the equation provides two solutions. The desired joint position must be chosen according to the physical limits of the joint and/or using additional criteria (e.g. comfort, least change).

i) Positioning the wrist

To move the arm wrist to a given position, P, in space, we need to determine the corresponding values of θ_1, θ_2, θ_3 and θ_4. Given the kinematics of our anthropomorphic arm, the distance, ρ, from the base to the wrist depends only on θ_4. Using Equation (1), the following constraint holds:

$$a\cos(\theta_4) + b\sin(\theta_4) = \rho^2 - (a_2^2 + l_2^2 + l_1^2 + a_1^2)$$

where we have used:

$$\begin{cases} a &= 2(-a_2 a_1 + l_2 l_1) \\ b &= -2(l_2 a_1 + a_2 l_1) \end{cases}$$

The value of θ_4 is readily obtained applying Equation (2). To determine θ_2, we will use the expression related to the z component, in Equation (1). This equation provides a solution for θ_2, as well as a constraint on θ_3 to ensure that a solution to Equation (2) exists. Hence, we first define an initial value for θ_3 and solve for θ_2. Then, we can change the value of θ_3, within the prescribed limits, and re-calculate θ_2.

Having calculated θ_4, θ_2 and θ_3, we now have to determine θ_1. We first move all the terms in Equation (1) that depend on θ_1 and θ_2 to the left hand side, yielding:

$${}^2_1T\ {}^1_0T\ P = {}^2_3T\ {}^3_4T\ {}^4_5T\ {}^5_6T\ Z \qquad (3)$$

From Equation (3), we obtain two transcendental equations on θ_1, each providing two possible solutions for θ_1. The final value for θ_1 must be a solution to both equations.

In the beginning, θ_3 can be chosen freely, within the restriction for evaluating θ_2. However, for some choices for θ_3, it may be impossible to solve for θ_1 or, more commonly, the solution obtained may be outside the physical limits of the robot. When this occurs, a new value must be chosen for θ_3 and the whole process for solving for θ_2 and θ_1 repeated, until a solution is found. This problem occurs when we want to reach positions just in in front of the body. In such a case, we can use $\theta_3 = 90\frac{z}{l_2}$, as an initial condition.

Given the kinematic structure of of the anthropomorphic robot arm, we need to use four different joints to reach the desired position of the wrist. In some sense, this gives us some redundancy to overcome obstacles or to find comfortable positions for the arm. However, we are left with only two degrees of freedom to orient the hand.

ii) Reaching an orientation

In conventional manipulators, the problems of positioning and orienting the end-effector are decoupled: the first 3 DOFs allow to position the end-effector and the remaining 3 are used to establish the orientation. The use of an anthropomorphic arm, in combination with a hand, allows us to proceed differently. When grasping a tool, attaching objects, or in many other tasks, the human hand may be constrained to work on a given plane. It is seldom the case that a specific orientation is needed. The reason is that the hand itself provides the extra mobility that might be necessary.

In our work, we propose to use a process of inverse kinematics that will fix the orientation of the hand parallel to a given working plane, allowing the hand to rotate freely around an axis perpendicular to this plane. For this approach, we only need two DOFs, the angles θ_5 and θ_6.

Let $V_\pi = [v_1 v_2 v_3]^T$ be normal to the working plane, Π. Our problem is then to determine the angles θ_5 and θ_6, such that the hand becomes parallel to Π.

Let ${}^0_6R$ represent the orientation of the coordinate frame $\{6\}$ with respect to the arm basis, $\{0\}$. The columns of ${}^0_6R$ are the axes of the frame $\{6\}$, expressed in the arm basis frame. From Figure 2, we can observe that the $x-$axis of the frame $\{6\}$ is perpendicular to the hand palm. Hence, the problem of keeping the hand palm parallel to the plane Π can be re-stated as determining θ_5 and θ_6, to make the first column of ${}^0_6R$ equal to V_π.

$${}^0_6R \begin{bmatrix} 1 \\ 0 \\ 0 \end{bmatrix} = \begin{bmatrix} v_1 \\ v_2 \\ v_3 \end{bmatrix}$$

Since ${}^0_4R$ is already known, θ_6 and θ_5 can be determined from the equation above, completing the process of determining the inverse kinematics.

If, in addition to aligning the hand palm with the working plane, one wants to reach a specific orientation around the normal to this plane, the value for θ_3 must be chosen accordingly. As this implies searching in one parameter only, which has a small amplitude, this computation is very fast. In this case, θ_3 can no longer be used as a redundant DOF when driving the wrist to some specified position.

Figure 3 shows a solution for a vertical working plane (parallel to the robot torso). The different orientations for the hand are obtained by choosing different values for internal/external shoulder rotation (θ_3).

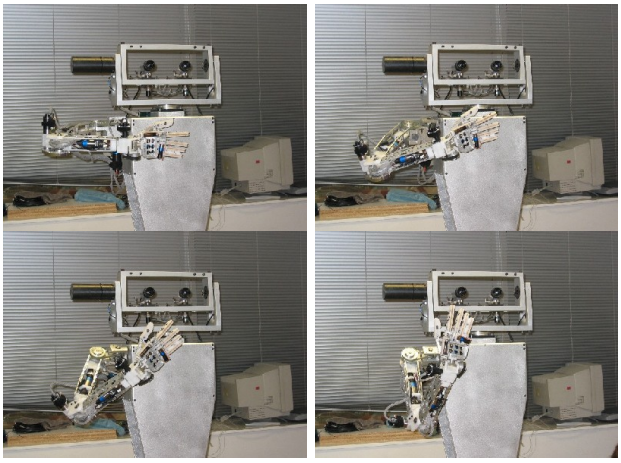

Fig. 3. Sequence of movements with the hand moving over a working plane, and changing the orientations, due to the change of θ_3

III. Design of an Anthropomorphic Robot Hand

Similarly to what we did with the arm, we start by providing a concise description of the human hand's anatomy, synthesized from [20], followed by the description of our robot hand.

A. The human hand anatomy

The hand is the organ of the human body that is most well adapted to prehensile function. The hand is composed of the palm and digits and is articulated to the forearm by the wrist (carpus). The palm is a flat surface that serves as the central support surface to the hand. The digits are composed of long bones called phalanges arranged in series continuing each metacarpal ray. The first digit, called the thumb, is composed of two phalanges; it is the most mobile of the digits and can oppose to the palm and the tips of the other fingers when these are flexed. The remaining four digits each contain 3 phalanges. Axial rotation (pronation-supination) of the hand occurs as the more mobile the two long bones of the forearm (the radius) rotates about the other relatively fixed bone (the ulna). The length, distribution and mobility of the digits with respect to the palm give the hand the ability to perform a wide variety of prehensile tasks.

The articulation connecting the digits to the metacarpals (MCP joint) allows for motion that is mostly independent of each other in flexion-extension and abduction-adduction (side-to-side motion). The thumb is different from the fingers in that it contains only 2 phalanges and its metacarpal bone has a wide range of motion where its base articulates with the carpus (i.e., thumb carpo-metacarpal, or CMC, joint). This makes the thumb the most independent and mobile of the digits. Its architectural and kinematic complexity separates the hand of man from other primates. The thumb occupies a special place in the digital pantheon.

The kinematics of the fingers have been approximated by rigid segments connected by ideal pin joints permitting ad-abduction and flexion-extension at the MCP joint, and flexion-extension at the proximal inter-phalangeal (PIP) and distal inter-phalangeal (DIP) joints.

The kinematics of the thumb are still not well understood. The large range of motion and mobility of the thumb has led to at least six different models in the literature.

The human hand nominally has 40 muscles classified as those located in the hand distal to the wrist (intrinsic muscles), and those located in the forearm (extrinsic muscles). Some tendons of the hand are atypical as they bifurcate or combine before inserting into bone to form the extensor mechanism (or extensor hood) of the fingers. The lumbrical muscle is atypical as it both originates from and inserts onto tendon (the flexor profundus tendon and the extensor hood, respectively) and has no direct bony attachment. Mammalian muscle tissue is considered to produce a maximal stress of $35N/cm^2$, which is a remarkable force/weight ratio difficult to match artificially.

B. Robot hand design

Our goal is to design an artificial hand capable of grasping objects and making gestures. Given the complexity of the human hand, we were forced to simplify the kinematics. In our robot hand, the index finger has three DOFs. The thumb has two DOFs plus one rotation and the other fingers have two DOFs. The pinkie and anelar fingers are mechanically coupled. The abductions were not implemented. The hand is shown in Figure 4.

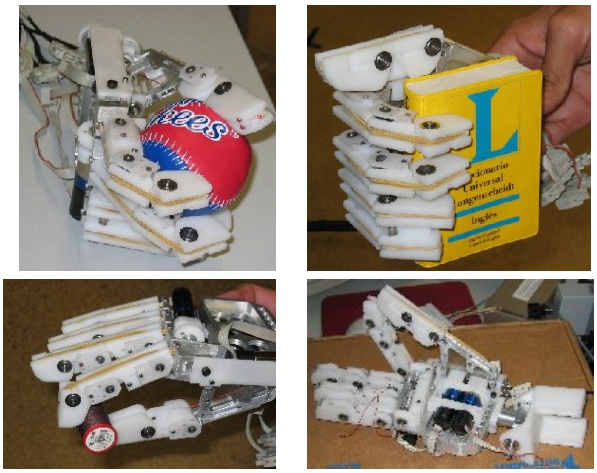

Fig. 4. Hand detail. Examples of grasping different objects.

One design constraint was to include all the motors on the hand. For this reason, we could not afford the space to use one independent motor for each joint in the fingers. The index finger is controlled by a single motor that pulls a tendon to close the finger. The thumb has two motors: one for rotation and another for closing the thumb by means of a tendon. The other three fingers have one motor/tendon mechanism that closes them all together.

At a first glance, the fact that not all the DOFs of each finger are controlled independently may seem very limiting. However, the finger joints are also strongly coupled in the human hand. In fact, our design gives some compliance to the robot hand, and makes the grasp control much easier, as the fingers adapt automatically to the shape objects. Without obstacles, the fingers start closing with the MCP joint. Figure 4 shows the hand grasping different types of objects.

The use of a single motor and a tendon to close a finger provides the hand with the ability to passively adapt to the objects shape. However, we need more proprioceptive information (in addition to motor shaft position) to know the state of the hand. The thumb, little and anelar fingers have one potentiometer as a position sensor, the middle and index have two potentiometers. In order to interact with objects, we installed pressure sensors in several places of the hand to measure contact forces.

IV. HEAD

The robot was equipped with a binocular robotic head [21], previously developed in our lab. It has four degrees of freedom: neck rotation, head elevation and independent eye vergence (see the kinematics in Figure 2). Manual adjustments can be made to align the vergence and elevation axes of rotation with the cameras optic centers. The inter-ocular distance can also be modified manually.

Table II shows the Modified Denavitt-Hartenberg parameters for the Medusa head.

Joint	a_{i-1}	α_{i-1}	d_i	θ_i
1	0	0	0	pan
2	-a	-90	0	$tilt$
3	0	-90	0	$verg$

TABLE II
MODIFIED DENAVITT-HARTENBERG PARAMETERS OF THE MEDUSA HEAD.

Let ${}^2P$ denote the $3D$ coordinates of point P, expressed in the eyes coordinates. If we denote by ${}^AP$, the coordinates of this point expressed in the arm base coordinate system, the following relation holds:

$$ {}^AP = {}^A_HT\, {}^0_1T_h\, {}^1_2T_h\, {}^2P $$

where the head-arm transformation, ${}^A_HT$, is given by:

$$ {}^A_HT = \begin{bmatrix} 0 & 0 & 1 & -27 \\ -1 & 0 & 0 & 0 \\ 0 & -1 & 0 & 29.6 \\ 0 & 0 & 0 & 1 \end{bmatrix} $$

This transformation allows to coordinate the head with the arm. Suppose that the arm is pointing towards the point ${}^0P = [x\, y\, z\, 1]^T$. This point can be represented in eye coordinates as: ${}^2P = [ed\, 0\, 0\, 1]^T$, where ed denotes the distance from the eye to the point. This equation can be used to determine the pan and $tilt$ angles to allow the head to look towards the same point.

Figure 5 shows several images where the head looks directly to the wrist, illustrating the head-arm coordination.

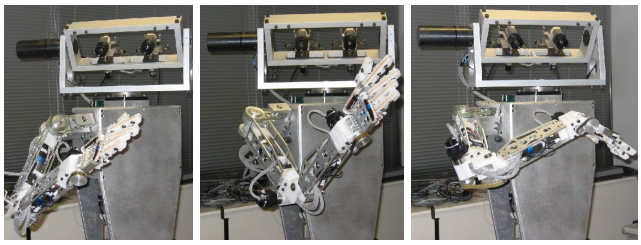

Fig. 5. Head/Hand Coordination example.

V. IMITATION

We will now show the ability of the robot to imitate the gestures, made by a person. These gestures will consist of arm movements in the air. Therefore, we need to track the demonstrator's arm, model the position and simultaneously reproduce the gesture with the robot arm. In this section we will present all the necessary steps to do this.

A. Vision system

Let $\mathbf{M} = [X\ Y\ Z]^T$ denote a 3D point expressed in camera coordinates. Then, with an orthographic camera model, $\mathbf{M}$ is projected onto $\mathbf{m} = [u\ v]^T$, according to:

$$ \begin{aligned} \mathbf{m} &= \mathcal{P}\mathbf{M} \\ \begin{bmatrix} u \\ v \end{bmatrix} &= s \begin{bmatrix} 1 & 0 & 0 \\ 0 & 1 & 0 \end{bmatrix} \begin{bmatrix} X \\ Y \\ Z \end{bmatrix} \end{aligned} \qquad (4) $$

where s is a scale factor that can be estimated placing a segment with size L fronto-parallel to the camera and measuring the image size l ($s = l/L$).

In order to model the arm position we have three steps of segmentation: background, person and hand.

The background is estimated by considering the intensity of each pixel, as a gaussian random variable, during initialization. We need about 100 frames to make a good model. After this process, we can estimate the probability of each pixel being part of the background. In order to increase the robustness of segmentation to illumination variations, we use RGB color scheme normalized with the blue channel.

The position of the person is estimated by template matching. A simple template allows to detect the We used pulleys of different radii in order to have the pinkie finger closing first. position of a person within an image. By scaling the template we can estimate the size of the person and the scale parameter, s, of the camera model. In addition, if we need to detect if the person is rotated with respect to the camera, we can scale the template independently in each direction, and estimate this rotation by the ratio between the head height and shoulder width.

To detect the hand, we used a skin-color segmentation process. Figure 6 shows a result of hand segmentation.

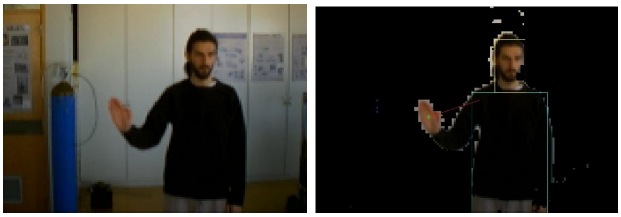

Fig. 6. Vision system. Left: original image. Right: background segmentation with human (the frame corresponds to the template matching) and hand detection.

B. Action-Level Imitation

If we assume that the movement of the hand is constrained to a plane or that the depth changes are small, we can use a simple view-point transformation to estimate the position of the person [22]. The system is able to imitate the tutor in real-time. Results are shown in Figure 7. When approaching singularities, the arm may exhibit some strange behavior. Nevertheless, this problem occurs only when the arm is aligned with the first joint, after which the shoulder moves upwards.

VI. CONCLUSIONS

We have presented the design of a (upper torso of a) humanoid robot consisting in a head, arm and hand. The

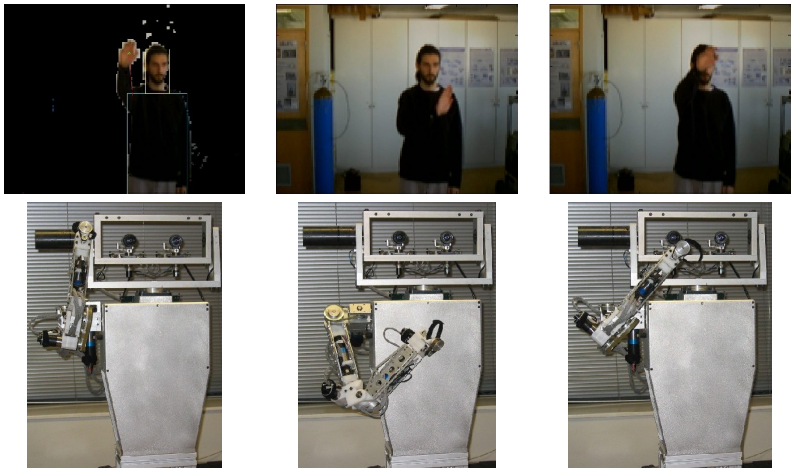

Fig. 7. Imitation of a persons movements

design goal was to build an experimental platform for research in imitation, learning and visuomotor coordination.

Research on imitation or visuomotor coordination in humanoid robotics is often hampered by the absence of adequate (and reasonably priced) experimental platforms. Most commercially available robot arms do not minimally meet the necessary criteria for this research.

We have shown that the anthropomorphic design may allow us generate more natural arm movements, by suitable defining the inverse kinematics. The additional flexibility arises from the anthropomorphic, integrated arm-hand design. In addition to providing the design options both for arm and hand, we present results on head-arm coordination and vision-based imitation, in real-time, to illustrate the usage of our robot.

We think that this research platform is very flexible and offers an extremely rich setup for research purposes. Since we believe that it may be of interest to many other research groups, we are currently considering the possibility of making it available to other laboratories around the world.

ACKNOWLEDGEMENTS

Work partially supported by: EU Proj. IST-2000-28159, MIRROR and by the FCT Programa Operacional Sociedade de Informação (POSI) in the frame of QCA III.

REFERENCES

[1] Neuronics. Katana. Technical report, http://www.neuronics.com/.

[2] T. Asfour, K. Berns, J. Schelling, and R. Dillman. Programming of manipulation tasks of the humanoid robot armar. In *International Conference on Advanced Robotics*, pages 25–27, Japan, 1999.

[3] Rodney Brooks, Cynthia Breazeal, Matthew Marjanovic, Brian Scassellati, and Matthew Williamson. *The Cog Project: Building a Humanoid Robot*, volume 1562. Springer-Verlag, computation for metaphors, analogy and agents edition, 1998.

[4] Giorgio Metta, Riccardo Manzotti, Francesco Panerai, and Giului Sandini. Babybot: an artificial developing robotic agent. In *SAB*, Paris, France, September 2001.

[5] Atsushi Konno, Noriyoshi Kato, Satoshi Shirata, Tomoyuki Furuta, and Masaru Uchiyama. Development of a light-weight biped humanoid robot. In *International Robots and Systems*, Japan, 2000.

[6] Akihiko Nagakubo, Yasuo Kuniyoshi, and Gordon Cheng. Development of a high-performance upper-body humanoid system. In *International Robots and Systems*, Japan, 2000.

[7] K. Nishiwaki, T. Sugihara, S. Kagami, F. Kanehiro, M. Inaba, and H.Inoue. Design and development of research platform for perception-action integration in humanoid robot: H6. In *International Robots and Systems*, Japan, 2000.

[8] Thomas B. Moeslund and Erik Granum. Modelling and estimating the pose of a human arm. *Machine Vision and Applications*, 14:237–247, 2003.

[9] Shadow Robot Company Rich Walker. Design of a dextrous hand for advanced clawar applications. In *6th International Conference on Climbing and Walking Robots*, Catania, Italy, 2003.

[10] Naoki Fukaya, Shigeki Toyama, Tamim Asfour, and Rudiger Dillman. Design of the tuat/karlsruhe humanoid hand. In *International Robots and Systems*, Japan, 2000.

[11] J. Butterfab et al. Dlr-hand ii: Next generation of a dextrous robot hand. In *ICRA*, pages 109–114, Korea, 2001.

[12] S. Schaal. Is imitation learning the route to humanoid robots. *Trends in Cognitive Sciences*, 3(6), 1999.

[13] Marcia Riley, Ales Ude, Keegan Wade, and Christopher G. Atkeson. Enabling real-time full-body imitation: A natural way of transferring human movement to humanoids. In *International Conference on Robotics and Automation*, pages 2368–2374, Taipei, Taiwan, 2003.

[14] Andrew H. Fagg. *A Computational Model of the Cortical Mechanisms Involved in Primate Grasping*. PhD thesis, University of Southern California, 1996.

[15] Erhan Oztop. *Modeling the Mirror: Grasp Learning and Action Recognition*. PhD thesis, University of Southern California, 2002.

[16] M. A. Arbib, A. Billard, M. Iacoboni, and E. Oztop. Synthetic brain imaging: grasping, mirror neurons and imitation. *Neural Networks*, 13:975–997, 2000.

[17] Aude Billard and Stephan Schaal. Robust learning of arm trajectories through human demonstration. In *IROS*, pages 734–739, Hawaii, USA, 2001.

[18] W. Maurel. *3D Modeling of the Human Upper Limb including the Biomechanics of Joints, Muscles and Soft Tissues*. PhD thesis, Laboratoire d'Infographie - EPFL - Lausanne, 1998.

[19] John J. Craig. *Introduction to Robotics*. Addison-Wesley, 1989.

[20] Francisco J. Valero-Cuevas and Vincent R. Hentz. Anatomy and physiology of the human hand. In *Workshop on Human and Machine Haptics*, California, USA, 1997.

[21] José Santos-Victor, Franc van Trigt, and João Sentieiro. Medusa - a stereo head for active vision. In *International Workshop on Intelligent Robotic Systems - IRS94*, Grenoble, France, 1994.

[22] Manuel Lopes and José Santos-Victor. Visual transformations in gesture imitation: What you see is what you do. In *ICRA*, pages 2375–2381, Taipei,Taiwan, 2003.